Disruption of Erk-dependent type I interferon induction breaks the myxoma virus species barrier

Fuan Wang[1], Yiyue Ma[1], John W Barrett[1], Xiujuan Gao[1], Joy Loh[2], Erik Barton[2], Herbert W Virgin IV[2] & Grant McFadden[1]

Myxoma virus, a member of the poxvirus family, causes lethal infection only in rabbits, but the mechanism underlying the strict myxoma virus species barrier is not known. Here we show that myxoma virus infection of primary mouse embryo fibroblasts elicited extracellular signal–regulated kinase (Erk) signaling, which was integrated to interferon regulatory factor 3 activation and type I interferon induction. We further show that Erk inactivation or disruption of interferon signaling mediated by the transcription factor STAT1 broke the cellular blockade to myxoma virus multiplication. Moreover, STAT1 deficiency rendered mice highly susceptible to lethal myxoma virus infection. Thus, the Erk–interferon–STAT1 signaling cascade elicited by myxoma virus in nonpermissive primary mouse embryo fibroblasts mediates an innate cellular barrier to poxvirus infection.

Poxviruses are large cytoplasmic DNA viruses that are of considerable medical and veterinary importance[1]. Myxoma virus is a member of the poxvirus family that causes a highly lethal disease known as myxomatosis in the European rabbit but does not infect any other vertebrate species[2,3]. Despite extensive advances in the understanding of poxvirus replication[4], so far the molecular basis underlying the strict species barrier for myxoma virus infection, or indeed any poxviruses, is still not well understood. Although myxoma virus does not infect mice, certain transformed mouse 3T3 clones are permissive to myxoma virus replication in a way that was originally ascribed to the expression of cell surface chemokine receptors[5] but was later shown to correlate with intracellular signaling of the kinase PAK1 (ref. 6). However, mouse cells have a propensity for genetic mutations during transformation[7] and it is often difficult to extrapolate the observations from transformed mouse cells to primary cells[8], which are generally regarded as having the closest resemblance to the *in vivo* cellular context[7]. Therefore, we explored using primary mouse embryo fibroblasts (pMEFs) as a model system for investigating the involvement of the cellular signaling pathways in the modulation of poxvirus host restriction. Productive virus infection depends heavily on viral ability to manipulate the cellular signaling machinery[9]. For example, the exploitation of mitogen-activated protein kinase (MAPK) extracellular signal–regulated kinase 1/2 (Erk1/2) signaling by many viruses constitutes an essential part of their replicative life cycles. Specifically, a variety of viruses, such as influenza virus, Borna disease virus, coxsackievirus, human immunodeficiency virus and vaccinia virus, have been shown to activate and 'co-opt' the Erk1/2 cascade during productive infection in permissive cells[9–13]. However, Erk1/2
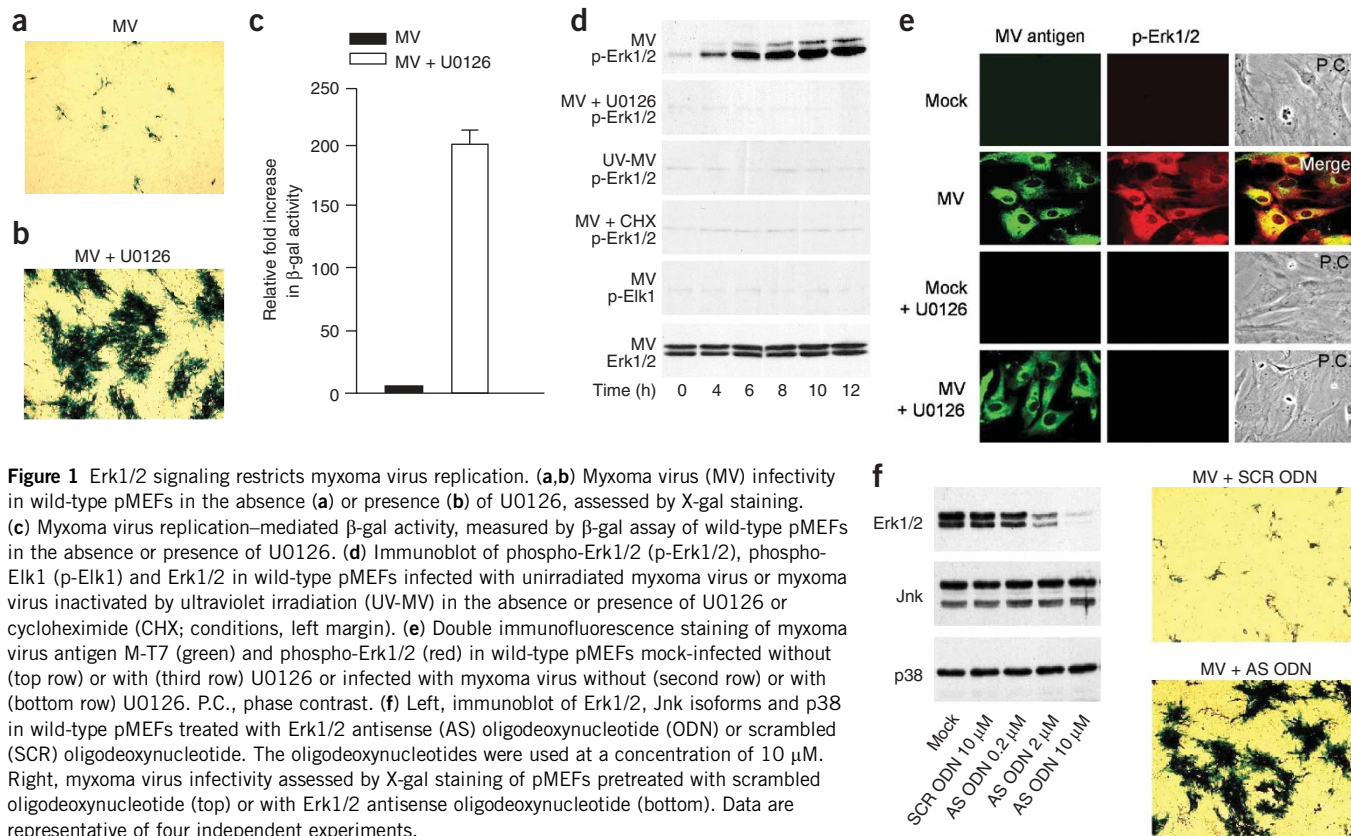
activation mediates the expression of an array of antiviral cytokines and chemokines, including various interleukins, the chemokine CCL5 (RANTES), type II interferon (IFN-γ) and tumor necrosis factor[9,14–17]. Although seemingly paradoxical, the apparently opposing effects of Erk1/2 signaling suggests that for certain viruses, the ultimate outcome of a viral infection is probably the result of a balance between proviral and antiviral signaling.

Type I interferon (IFN-α and IFN-β) is an important cytokine best characterized for its antiviral activity during the innate immune defense against invading viruses[18–20]. The expression of type I interferon requires multiple cellular transcription factors[21–23], especially interferon regulatory factor 3 (IRF3), whose activation is essential for the transcriptional initiation of the cytokine[24,25]. However, little if anything is known about whether Erk1/2 signaling is involved in regulating the expression of type I interferon. Virus-induced signaling pathways that can be integrated to the IRF3 activation loop remain to be fully explored, particularly after virus infection of nonpermissive cells.

Here we provide evidence that Erk1/2 signaling operates 'upstream' of IRF3 activation to induce type I interferon expression after myxoma virus infection of nonpermissive pMEFs. We further show that disruption of this signaling cascade of Erk1/2, interferon and the transcription factor STAT1 renders the normally resistant pMEFs fully permissive to myxoma virus multiplication and that mice defective in STAT1 signaling become highly susceptible to lethal myxoma virus infection. Our data provide new insights into the molecular basis for myxoma virus species barrier and also show a previously unrecognized link between Erk1/2 signaling and type I interferon induction.

[1]Robarts Research Institute, and Department of Microbiology and Immunology, The University of Western Ontario, London, Ontario N6G 2V4, Canada. [2]Department of Pathology and Immunology and Department of Molecular Microbiology, Washington University School of Medicine, St. Louis, Missouri 63110, USA. Correspondence should be addressed to G.M. (mcfadden@robarts.ca).

Figure 1 Erk1/2 signaling restricts myxoma virus replication. (**a,b**) Myxoma virus (MV) infectivity in wild-type pMEFs in the absence (**a**) or presence (**b**) of U0126, assessed by X-gal staining. (**c**) Myxoma virus replication–mediated β-gal activity, measured by β-gal assay of wild-type pMEFs in the absence or presence of U0126. (**d**) Immunoblot of phospho-Erk1/2 (p-Erk1/2), phospho-Elk1 (p-Elk1) and Erk1/2 in wild-type pMEFs infected with unirradiated myxoma virus or myxoma virus inactivated by ultraviolet irradiation (UV-MV) in the absence or presence of U0126 or cycloheximide (CHX; conditions, left margin). (**e**) Double immunofluorescence staining of myxoma virus antigen M-T7 (green) and phospho-Erk1/2 (red) in wild-type pMEFs mock-infected without (top row) or with (third row) U0126 or infected with myxoma virus without (second row) or with (bottom row) U0126. P.C., phase contrast. (**f**) Left, immunoblot of Erk1/2, Jnk isoforms and p38 in wild-type pMEFs treated with Erk1/2 antisense (AS) oligodeoxynucleotide (ODN) or scrambled (SCR) oligodeoxynucleotide. The oligodeoxynucleotides were used at a concentration of 10 μM. Right, myxoma virus infectivity assessed by X-gal staining of pMEFs pretreated with scrambled oligodeoxynucleotide (top) or with Erk1/2 antisense oligodeoxynucleotide (bottom). Data are representative of four independent experiments.

RESULTS

Erk1/2 signaling mediates myxoma virus cellular restriction

To examine myxoma virus infectivity in primary mouse cells, we infected wild-type pMEFs with a myxoma virus derivative expressing β-galactosidase (β-gal) under the control of a late viral promoter. Myxoma virus was unable to produce the classic permissive blue foci in this assay but instead induced only isolated blue cells, indicating that myxoma virus replication had proceeded to the stage of late viral gene expression before the infection prematurely aborted (**Fig. 1a**).

The abortive nature of this myxoma virus infection led us to hypothesize that the cellular restriction of myxoma virus replication might be due to the inability of myxoma virus to initiate an appropriate intracellular signaling environment in pMEFs. To test this hypothesis, we screened a variety of signaling modulators and discovered that the MEK inhibitor U0126 was able to reverse the nonpermissive myxoma virus phenotype of pMEFs to the fully permissive phenotype (**Fig. 1b**). Quantitatively, U0126 treatment resulted in an increase of about 200-fold in myxoma virus replication–mediated β-gal activity (**Fig. 1c**).

U0126 shows high specificity[26] and is now a widely used agent for the specific inhibition of Erk1/2 signaling[10–12]. Hence, the results presented above seem rather unexpected, as Erk1/2 activation has been reported to be essential for viral replication for many viruses including vaccinia virus[9–13]. To ensure that U0126 inhibits myxoma virus–elicited Erk1/2 activation in nonpermissive pMEFs, we examined Erk1/2 status by immunoblot with an antibody to phosphorylated Erk1/2 (phospho-Erk1/2). Myxoma virus infection triggered prolonged Erk1/2 phosphorylation, which became detectable 4 h after infection (**Fig. 1d**, top), whereas Erk1/2 protein expression remained unaltered during the infection (**Fig. 1d**, bottom). As shown by immunoblot, U0126 completely abrogated myxoma virus–elicited Erk1/2 phosphorylation (**Fig. 1d**, second panel). The potency of U0126 inhibition was further confirmed by the lack of specific immunostaining for phospho-Erk1/2 in either control or myxoma virus–infected cells pretreated with U0126 (**Fig. 1e**, third and bottom rows).

To explore the myxoma virus–elicited Erk1/2 signaling properties, we first determined whether myxoma virus binding alone was involved in Erk1/2 activation by infecting pMEFs with myxoma virus inactivated by ultraviolet irradiation. Virus inactivated by ultraviolet irradiation failed to induce Erk1/2 phosphorylation (**Fig. 1d**, third panel). We then infected cells with myxoma virus in the presence of the protein inhibitor cycloheximide and found that the inhibition of *de novo* viral protein synthesis abolished myxoma virus–induced Erk1/2 phosphorylation (**Fig. 1d**, fourth panel). These results therefore suggest that myxoma virus gene expression is required for the induction of Erk1/2 phosphorylation in pMEFs. To define the consequences of myxoma virus–activated Erk1/2, we examined the phosphorylation status of the prototypic Erk1/2 substrate Elk1, a transcription factor that resides exclusively in the nucleus[27,28]. Elk1 phosphorylation is often used as a 'readout' for the nuclear signal transduction relayed by activated Erk1/2 (refs. 27,28). Elk1 was not phosphorylated (**Fig. 1d**, fifth panel), despite the fact that Erk1/2 was strongly activated by myxoma virus infection in pMEFs. This finding suggested that myxoma virus–activated Erk1/2 might fail to translocate into the nucleus. To confirm this, we examined the subcellular localization of the kinase by immunofluorescence microscopy; phosphorylated Erk1/2 was indeed localized mainly in the cytoplasm of myxoma virus–infected pMEFs (**Fig. 1e**, second row). Thus, these results showed an unexpected Erk1/2 signaling pattern[27–29].
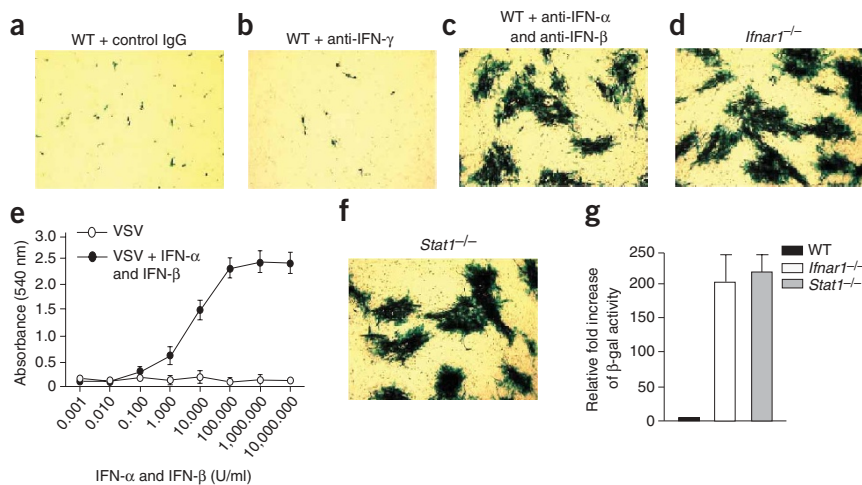
Figure 2 Type I interferon induction mediates the cellular restriction of myxoma virus replication. (a–d) Myxoma virus infectivity assessed by X-gal staining of wild-type (WT) pMEFs treated with normal sheep IgG (a), anti-IFN-γ (b) or anti–IFN-α and IFN-β (c), or in *Ifnar1*^{−/−} pMEFs (d). (e) Uptake of vital dye crystal violet assessed by spectroscopy of wild-type pMEFs without pretreatment or pretreated with IFN-α and IFN-β. VSV, vesicular stomatitis virus. (f) Myxoma virus infectivity assessed by X-gal staining of *Stat1*^{−/−} pMEFs. (g) Myxoma virus replication–mediated β-gal activity in *Ifnar1*^{−/−} pMEFs and *Stat1*^{−/−} pMEFs assessed by β-gal assay. Data are representative of four independent experiments.

To determine the correlation between myxoma virus infection and Erk1/2 activation at the cellular level, we used immunofluorescence colocalization of the myxoma virus antigen M-T7, encoded by an early myxoma virus gene[30], with cellular phosphorylated Erk1/2. Erk1/2 phosphorylation correlated well with actual intracellular myxoma virus infection (**Fig. 1e**, second row). These findings thus indicate that myxoma virus infection triggered Erk1/2 activation.

As an independent method to verify the function of Erk1/2 in the determination of myxoma virus infectivity, we attempted to deplete Erk1/2 in pMEFs using Erk1/2 antisense oligodeoxynucleotides, a well established means for suppressing Erk1/2 signaling in various systems, including primary cells[31,32]. Erk1/2 'knockdown' by the antisense oligodeoxynucleotides was dose dependent (**Fig. 1f**, left). At an oligodeoxynucleotide concentration of 10 μM, Erk1/2 protein was depleted considerably after 60 h, whereas the expression of two other MAPKs, p38 and Jnk (isoforms p46 and p54), remained unaltered. Plaque assay further demonstrated that Erk1/2 depletion by the antisense treatment rendered the resistant pMEFs fully permissive to myxoma virus proliferation (**Fig. 1f**, right), consistent with what we noted with U0126 (**Fig. 1b**). The findings above show that myxoma virus infection of nonpermissive pMEFs elicits a specific noncanonical Erk1/2 signaling pattern that is essential for maintaining the cellular restriction of productive myxoma virus infection.

Myxoma virus infection induces type I interferon

The findings presented above suggest that certain cellular gene products whose myxoma virus–inhibitory effect is related to Erk1/2

activation are key in maintaining the cellular nonpermissivity of pMEFs to myxoma virus infection. As viral infection often induces type I interferon[18,23], a potent antiviral molecule, we therefore reasoned that the best candidate for such a virus-inhibiting cellular product was type I interferon induced by myxoma virus infection of pMEFs.

To test this hypothesis, we first did type I interferon neutralization assays. Although sporadic blue cells were discernible at a low multiplicity of infection (MOI) of 0.01 in groups treated with control immunoglobulin G (IgG) or antibody to IFN-γ (anti-IFN-γ) (**Fig. 2a,b**), the same amount of input myxoma virus yielded large canonical blue foci in type I interferon–neutralized pMEFs (**Fig. 2c**). Furthermore, there was fully permissive myxoma virus replication in pMEFs deficient in type I interferon receptor (*Ifnar1*^{−/−}; **Fig. 2d**). These results thus convincingly demonstrate that type I interferon is responsible for keeping pMEFs in the nonpermissive state against myxoma virus proliferation. The isolated blue cells seen with infection of wild-type pMEFs at the low MOI strongly suggest that the type I interferon produced from the initially myxoma virus–infected cells protected the neighboring naive cells from the subsequent myxoma virus infection. To further confirm the effect of type I interferon on pMEFs, we pretreated the cells with IFN-α and IFN-β for 24 h and then challenged them with interferon-sensitive vesicular stomatitis virus. Vesicular stomatitis virus was able to infect pMEFs, whereas the interferon-pretreated pMEFs were nonpermissive to infecting vesicular stomatitis virus in a dose-dependent way (**Fig. 2e**).

Next we examined the function of STAT1 in myxoma virus–induced type I interferon signaling because STAT1 is a pivotal transducing
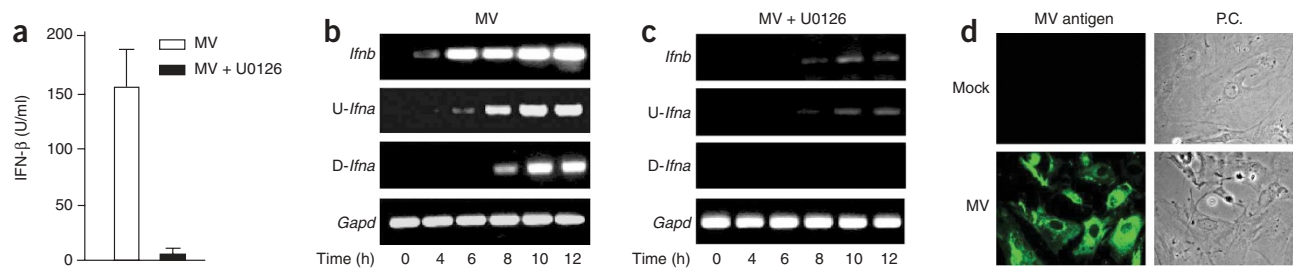

Figure 3 Erk1/2 signaling is required for optimal induction of type I interferon. Wild-type pMEFs were infected with myxoma virus in the absence or presence of U0126. (a) IFN-β accumulation in the culture supernatants assessed by standard sandwich ELISA. (b,c) Total RNA analyzed by RT-PCR for induction of IFN-β (*Ifnb*), universal IFN-α (U-*Ifna*) and delayed IFN-α (D-*Ifna*). *Gapd*, glyceraldehyde phosphodehydrogenase (control). (d) Visualization of myxoma virus infection–specific antigen M-T7 by immunofluorescence staining (green) with the same infection conditions used for RT-PCR. P.C., phase contrast. Data are representative of four independent experiments.
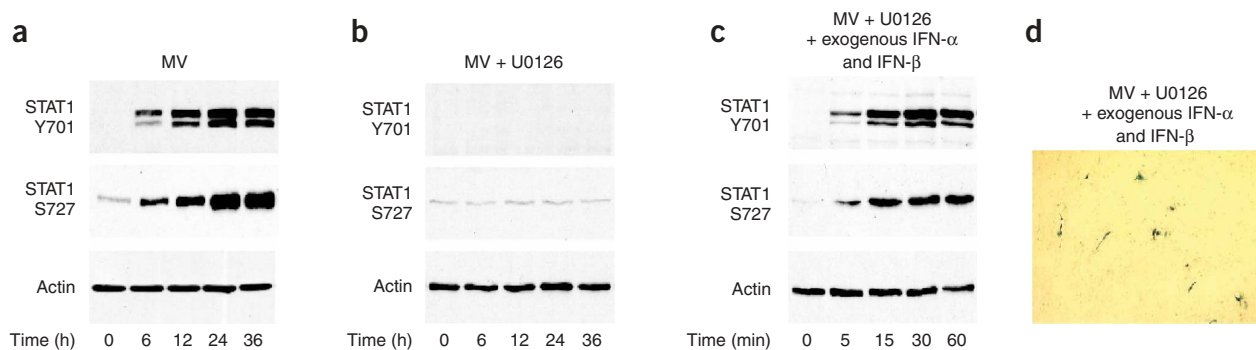
Figure 4 STAT1 activation by type I interferon does not require Erk1/2 participation. (**a–c**) Immunoblot of phospho-STAT1 (Y701 and S727) in myxoma virus–infected wild-type pMEFs in the absence (**a**) or presence (**b**) of U0126, or in myxoma virus–infected pMEFs with the concurrent presence of U0126 and exogenous IFN-α and IFN-β (**c**). (**d**) Myxoma virus infectivity determined by X-gal staining of pMEFs treated with U0126 and exogenous IFN-α and IFN-β. Data are representative of five independent experiments.

molecule downstream of interferon receptor ligand engagement and is essential in mediating interferon's antiviral effects[18,20,33]. STAT1 deficiency rendered the previously restrictive pMEFs fully permissive to myxoma virus replication (**Fig. 2f**). Quantitatively, a β-gal assay showed that both STAT1 and interferon receptor deficiencies promoted myxoma virus replication to a similar extent (**Fig. 2g**) that was comparable to that achieved by Erk1/2 inactivation in wild-type pMEFs (**Fig. 1c**). These data unequivocally demonstrate that the central element restricting myxoma virus replication in pMEFs is the STAT1-dependent type I interferon response triggered by myxoma virus infection itself.

Type I interferon expression is Erk1/2 dependent

Our finding that type I interferon response can mediate the same level of cellular restriction for myxoma virus replication as that imposed by Erk1/2 activation in the nonpermissive pMEFs (**Figs. 1c** and **2g**) suggest that these two distinct signaling cascades may be interrelated in orchestrating the cellular blockade to myxoma virus proliferation. Therefore, to investigate whether these two pathways intersect, we first measured IFN-β production in pMEFs after myxoma virus infection in the presence or absence of U0126. Myxoma virus infection resulted in substantial IFN-β production in pMEFs (**Fig. 3a**). In contrast, pretreatment with U0126 substantially suppressed myxoma

virus–induced IFN-β secretion (**Fig. 3a**). Next, to determine whether the inhibition of myxoma virus–induced type I interferon response is at the transcriptional level, we assessed IFN-α and IFN-β induction by RT-PCR using primers for IFN-β, consensus sequence primers for all subtypes of IFN-α ('universal IFN-α') and non-IFN-α4 sequence primers for only delayed subtypes of IFN-α ('delayed IFN-α'). Both IFN-β and universal IFN-α mRNA was highly induced with similar kinetics after myxoma virus infection (**Fig. 3b**), whereas delayed IFN-α mRNA was induced later. However, when pMEFs were infected with myxoma virus inactivated by ultraviolet irradiation, IFN-α and IFN-β mRNA expression was not induced (data not shown). These results thus indicate that, as for Erk1/2 activation, myxoma virus binding alone was not a sufficient stimulus for IFN induction. Next, we examined IFN-α and IFN-β induction in the presence of U0126. Inactivation of Erk1/2 signaling substantially reduced the expression of both IFN-β and universal IFN-α mRNA, whereas delayed IFN-α mRNA induction was essentially abolished (**Fig. 3c**). Thus, Erk1/2 signaling is required for the optimal induction of type I interferon in response to myxoma virus infection of nonpermissive pMEFs.

To determine whether type I interferon induction actually occurred in myxoma virus–infected cells, we examined the intracellular myxoma virus infection status by immunofluorescence microscopy of M-T7, the early viral antigen specific for myxoma virus infection[30].
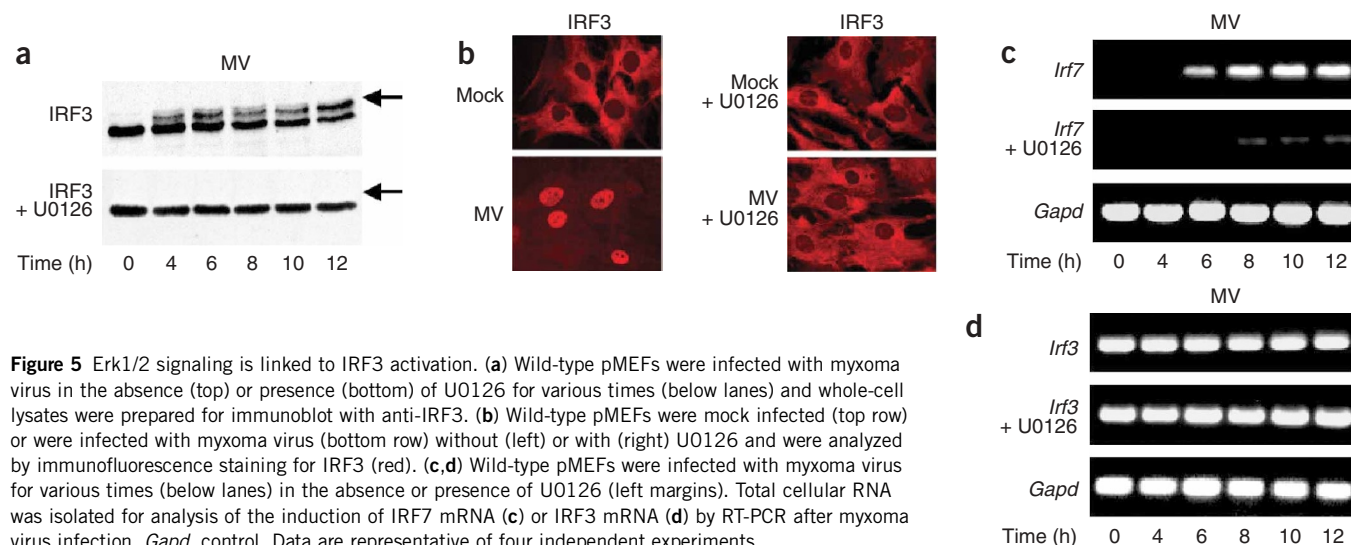

Figure 5 Erk1/2 signaling is linked to IRF3 activation. (**a**) Wild-type pMEFs were infected with myxoma virus in the absence (top) or presence (bottom) of U0126 for various times (below lanes) and whole-cell lysates were prepared for immunoblot with anti-IRF3. (**b**) Wild-type pMEFs were mock infected (top row) or were infected with myxoma virus (bottom row) without (left) or with (right) U0126 and were analyzed by immunofluorescence staining for IRF3 (red). (**c,d**) Wild-type pMEFs were infected with myxoma virus for various times (below lanes) in the absence or presence of U0126 (left margins). Total cellular RNA was isolated for analysis of the induction of IRF7 mRNA (**c**) or IRF3 mRNA (**d**) by RT-PCR after myxoma virus infection. *Gapd*, control. Data are representative of four independent experiments.

ARTICLES

Figure 6 Myxoma virus infection elicits PKR-independent, STAT1-mediated eIF2α phosphorylation. (**a**) Wild-type pMEFs were infected with myxoma virus alone or in the presence of U0126 (left margin) for various time periods (below lanes). Whole-cell lysates were prepared for immunoblot of phospho-eIF2α (eIF2α S51), phospho-PKR (PKR T451) and PKR (PKR protein). (**b,c**) Myxoma virus infectivity determined by X-gal staining of *Prkr*⁻/⁻ pMEFs infected with myxoma virus in the absence (**b**) or presence (**c**) of U0126. (**d**) *Prkr*⁻/⁻ pMEFs were infected with myxoma virus with or without U0126 (left margin) for various times (below lanes) and whole-cell lysates were prepared for immunoblot of phospho-eIF2α, phospho-PKR and PKR. (**e**) Myxoma virus infectivity assessed by X-gal staining of *Prkr*⁻/⁻ *Stat1*⁻/⁻ pMEFs. (**f**) *Prkr*⁻/⁻ *Stat1*⁻/⁻ pMEFs were infected with myxoma virus for various times (below lanes) and whole-cell lysates were prepared for immunoblot of phospho-eIF2α, phospho-PKR and PKR. Data are representative of three independent experiments.
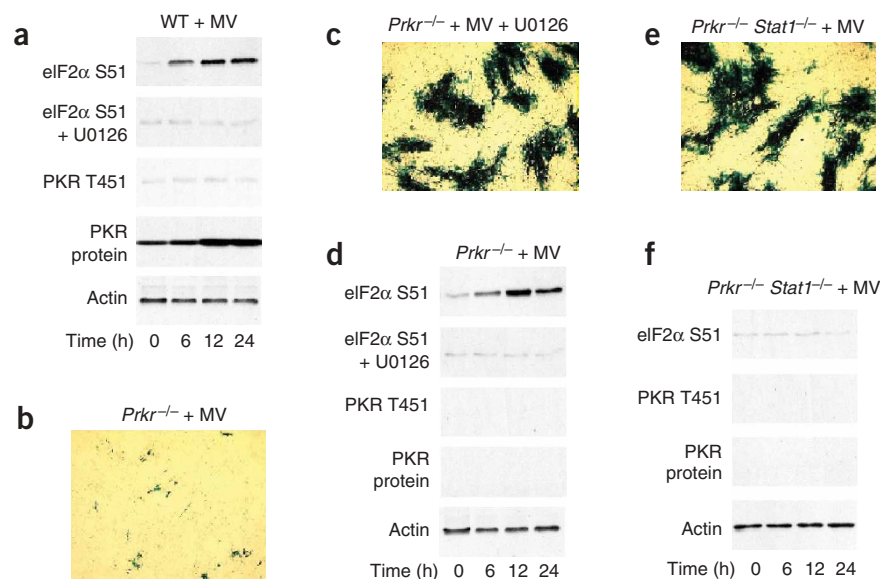
Almost all the pMEFs were positive for M-T7 at the MOI used for the RT-PCR assays at 12 h after infection (**Fig. 3d**), at which time the lysates were prepared for RNA isolation. Thus, type I interferon was induced in myxoma virus–infected pMEFs. Erk1/2 inactivation impairs STAT1-mediated type I interferon signal transduction[34]. To ascertain whether STAT1 activation is also Erk1/2 dependent in the myxoma virus–pMEF system, we examined the phosphorylation status of STAT1 by immunoblot. STAT1 was phosphorylated at both tyrosine (Y701) and serine (S727) residues after myxoma virus infection (**Fig. 4a**). In contrast, STAT1 phosphorylation was completely suppressed when Erk1/2 was inhibited by U0126 during myxoma virus infection (**Fig. 4b**). Because U0126 inhibited type I interferon production (**Fig. 3a**), the lack of STAT1 phosphorylation after myxoma virus infection in U0126-pretreated pMEFs can be attributed to the lack of interferon required to initiate signaling from interferon receptors to STAT1. To further verify this, we challenged the U0126-pretreated pMEFs simultaneously with myxoma virus and exogenous type I interferon. STAT1 was activated normally by the exogenously added type I interferon in the case of Erk1/2 inactivation in myxoma virus–infected cells (**Fig. 4c**). Moreover, Erk1/2 inactivation by U0126 was no longer able to reverse the restrictive myxoma virus phenotype when exogenous type I interferon was supplemented in the infection medium (**Fig. 4d**). Thus, these data further show that type I interferon induction, not STAT1 activation, is Erk1/2 dependent after myxoma virus infection in pMEFs.

Myxoma virus–elicited Erk1/2 activation and IRF3
The link between Erk1/2 signaling and type I interferon gene induction prompted us to examine how these pathways intersect. Phosphorylated Erk1/2 was localized mainly in the cytoplasm of myxoma virus–infected pMEFs (**Fig. 1e**, second row). This localization pattern may be important, because IRF3, a central mediator of the transcriptional initiation of type I interferon, is a preexisting latent cytoplasmic protein[22,24,35,36] and translocates to the nucleus only after being phosphorylated in the cytoplasm. Therefore, we postulated that in myxoma virus–infected pMEFs, Erk1/2 signaling and the type I interferon response might converge on IRF3 activation. To test this, we examined IRF3 activation status after myxoma virus infection. Myxoma virus infection of nonpermissive pMEFs led to rapid IRF3

phosphorylation, as showed by a retarded shift in mobility of IRF3 bands by SDS-PAGE[35,37] (**Fig. 5a**, top). Immunofluorescence microscopy further demonstrated that IRF3 translocated into the nucleus in the myxoma virus–infected cells, indicative of IRF3 activation (**Fig. 5b**, left). Phosphorylation of IRF3, however, was completely abrogated when Erk1/2 was inactivated by U0126, as shown by the absence of the more slowly migrating forms of IRF3 (**Fig. 5a**, bottom) and the concurrent inhibition of IRF3 nuclear translocation (**Fig. 5b**, right). These findings show that myxoma virus–elicited Erk1/2 induces IRF3 activation in pMEFs after myxoma virus infection. In addition to IRF3, IRF7 has an important synergistic function in the transcriptional regulation of type I interferon, especially the delayed subtypes of IFN-α[21,24,38]. Therefore, we investigated IRF7 signaling profiles after myxoma virus infection of nonpermissive pMEFs. Unlike IRF3, IRF7 protein was not detectable in uninfected pMEFs (data not shown). Consequently, we examined IRF7 mRNA in pMEFs after myxoma virus infection. RT-PCR showed that IRF7 mRNA was not expressed in the control cells but was notably induced by myxoma virus infection (**Fig. 5c**, top). In contrast, IRF7 mRNA induction was inhibited considerably by U0126-mediated Erk1/2 inactivation (**Fig. 5c**, middle). Preexisting IRF3 mRNA remained unaltered during myxoma virus infection, irrespective of Erk1/2 status (**Fig. 5d**). Hence, these findings indicate that the inhibition of IRF7 signaling by Erk1/2 inactivation occurs at the transcriptional level.

Myxoma virus induces PKR-independent eIF2α phosphorylation
Increasing evidence shows that phosphorylation of serine 51 (S51) of the α-subunit of eukaryotic translation initiation factor 2 (eIF2α) represents a chief point of control over the translation initiation in the viral replication blockade induced by IFN signaling[18,33,39]. To determine the effector(s) that exerted the antiviral activity induced by Erk1/2-dependent IFN response, we examined the status of eIF2α S51 after myxoma virus infection by immunoblot with a phospho-specific antibody. Phosphorylation of eIF2α S51 was increased considerably after myxoma virus infection in restrictive pMEFs (**Fig. 6a**, top) but was blocked by Erk1/2 inactivation (**Fig. 6a**, second panel).This result would suggest that PKR should be involved, as PKR has been extensively defined as a key eIF2α S51 kinase in the context of viral infection[18,33,39,40]. To formally ascertain whether PKR is the upstream
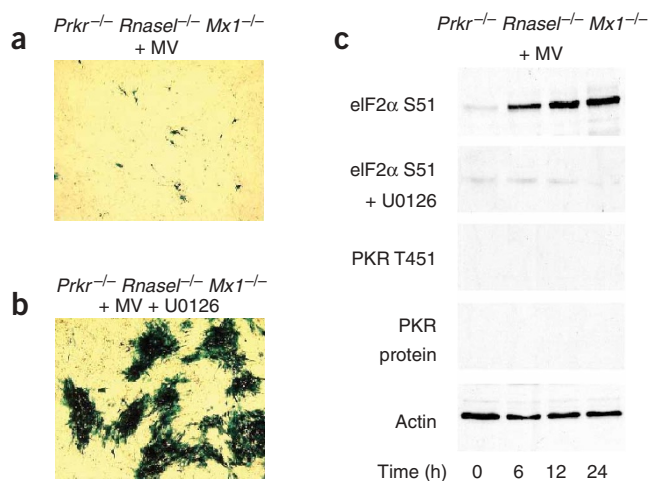

© 2004 Nature Publishing Group http://www.nature.com/natureimmunology

Figure 7 PKR, RNase L and Mx1 are not involved in Erk1/2-induced cellular restriction of myxoma virus multiplication. (**a,b**) Myxoma virus infectivity assessed by X-gal staining of $Prkr^{-/-}Rnasel^{-/-}Mx1^{-/-}$ pMEFs infected with myxoma virus in the absence (**a**) or presence (**b**) of U0126. (**c**) $Prkr^{-/-}Rnasel^{-/-}Mx1^{-/-}$ pMEFs were infected with myxoma virus for various times (below lanes) in the absence or presence of U0126 (left margin) and whole-cell lysates were prepared for immunoblot of phospho-eIF2α, phospho-PKR and PKR. Data are representative of four independent experiments.
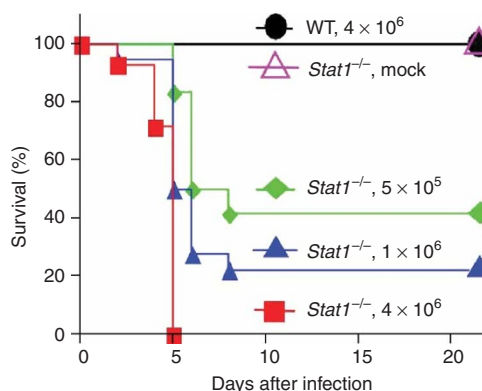

Figure 8 STAT1 deficiency renders mice highly susceptible to lethal myxoma virus infection. Wild-type mice ($n = 20$) were infected intracranially with myxoma virus at a dose of 4×10^6 plaque-forming units (PFU); $Stat1^{-/-}$ mice were given an intracranial injection of mock virus preparation ($n = 5$) or a single intracranial myxoma virus injection of 4×10^6 PFU ($n = 14$), 1×10^6 PFU ($n = 18$) or 5×10^5 PFU ($n = 12$). The infected mice were monitored for survival for 21 d. Data are representative of two independent experiments.

kinase for the observed phosphorylation of eIF2α S51, we examined phosphorylation of PKR T451 in myxoma virus–infected pMEFs at various times after infection. Unexpectedly, myxoma virus infection did not cause any appreciable increase in phosphorylation of PKR T451 beyond the low basal activity (**Fig. 6a**, third panel), despite the fact that pMEFs had high endogenous expression of PKR protein (**Fig. 6a**, fourth panel). These findings demonstrated that myxoma virus–elicited eIF2α S51 phosphorylation occurred without PKR activation in restrictive pMEFs. To further verify this, we assessed myxoma virus infectivity in PKR-deficient ($Prkr^{-/-}$) pMEFs and found that the $Prkr^{-/-}$ cells were highly resistant to myxoma virus infection (**Fig. 6b**). As with the wild-type counterparts, the restrictive myxoma virus phenotype was fully reversed in $Prkr^{-/-}$ pMEFs by U0126-mediated Erk1/2 inactivation (**Fig. 6c**). In the same way, phosphorylation of eIF2α S51 was augmented substantially in $Prkr^{-/-}$ pMEFs after myxoma virus infection but was blocked by U0126-mediated Erk1/2 inactivation (**Fig. 6d**).

Next, we examined the function of STAT1 signaling in the context of PKR deficiency by challenging $Prkr^{-/-}Stat1^{-/-}$ pMEFs with myxoma virus. STAT1 disruption rendered the previously resistant $Prkr^{-/-}$ pMEFs fully permissive to myxoma virus proliferation (**Fig. 6e**). Furthermore, in contrast to the prominent phosphorylation of eIF2α S51 in the nonpermissive $Prkr^{-/-}$ pMEFs, no activation of eIF2α S51 could be detected in the permissive $Prkr^{-/-}Stat1^{-/-}$ cells (**Fig. 6f**). These findings thus indicate that phosphorylation of eIF2α S51 is mediated by PKR-independent STAT1 signaling in myxoma virus–infected pMEFs. The preceding demonstration of PKR-independent antiviral response that restricts myxoma virus multiplication in pMEFs prompted us to further investigate any possible involvement of two other well defined interferon antiviral effectors: RNase L and Mx1 (refs. 18,33). To address whether PKR, RNase L or Mx1 has any compensatory functions, we examined myxoma virus infectivity in $Prkr^{-/-}Rnasel^{-/-}Mx1^{-/-}$ pMEFs. $Prkr^{-/-}Rnasel^{-/-}Mx1^{-/-}$ cells were resistant to myxoma virus

infection and showed no appreciable reduction at all in their anti-myxoma virus capacity (**Fig. 7a**), whereas Erk1/2 suppression by U0126 rendered them fully permissive to myxoma virus replication (**Fig. 7b**). Moreover, phosphorylation of eIF2α S51 was unaffected by the combined deficiency in PKR, RNase L and Mx1, but was ablated by Erk1/2 inactivation with U0126 (**Fig. 7c**). These findings show that Erk1/2-dependent STAT1-mediated phosphorylation of eIF2α S51 correlates well with the cellular restriction for myxoma virus infection in pMEFs. Furthermore, the restrictive pMEFs inhibit myxoma virus replication in a STAT1-dependent way, but entirely independent of PKR, RNaseL and Mx1.

STAT1 restricts myxoma virus infection in mice
The results presented so far have demonstrated that the molecular basis of the cellular restriction for myxoma virus proliferation in nonpermissive pMEFs is mediated by Erk1/2-dependent type I interferon induction. Furthermore, we have also shown that downstream of the type I interferon induction, the anti–myxoma virus effect is mediated by STAT1. To determine the *in vivo* physiological importance of this STAT1-mediated antiviral signaling, we challenged $Stat1^{-/-}$ mice with intracranial myxoma virus injection. $Stat1^{-/-}$ mice were highly susceptible to myxoma virus infection, and all the myxoma virus–infected knockout mice died within 5 d of infection after a single injection of 4×10^6 plaque-forming units. In contrast, wild-type mice were completely resistant (**Fig. 8**). Thus, these data show that myxoma virus pathogenesis is profoundly affected by STAT1 signaling, which is essential for maintaining the myxoma virus species barrier in mice.

DISCUSSION
The virus-host species barrier is a key determinant of viral pathogenesis. For many viruses this restriction is determined by species-specific receptor interactions[41]; however, the search for specific host receptors to rationalize the species specificities of poxviruses has been uniformly unrewarding[4]. In this study, we have shown that the molecular basis for the myxoma virus species barrier is mediated intracellularly by Erk1/2 signaling, which translates functionally into IRF3 activation and type I interferon expression, whose antiviral effect is mediated

downstream by STAT1. Thus, Erk1/2-IFN-STAT1 signaling cascade represents a mechanism by which the innate cellular barrier to restrict cross-species poxvirus infection can be explained.

Type I interferon consists of a single IFN-β and at least 12 different IFN-α subtypes in both mouse and human cells[18,38]. Although the early-phase induction of IFN-β and IFN-α4 is mediated by IRF3, the late-phase induction of non-IFN-α4 subtypes is reliant on IRF7 (refs. 24,38). Furthermore, *Irf7* is normally dormant in most cell types and is expressed only after stimulation by the first wave of IFN-β and IFN-α4 expression[21,38]. Here, inactivation of myxoma virus–elicited Erk1/2 signaling considerably reduced IRF7 expression and induction of the delayed IFN-α subtypes was abolished. Accordingly, the inhibitory effect on IRF7 signaling by Erk1/2 inactivation can be interpreted as being secondary to the blockade of IRF3-mediated early interferon action. Nonetheless, the combined effects contribute together to the profound inhibition of type I interferon expression. These results further emphasize the central involvement of IRF3 in the transcriptional regulation of type I interferon expression.

Our discovery of the myxoma virus–elicited signal transduction from Erk1/2 to IRF3 in nonpermissive pMEFs indicates several potential scenarios in which IRF3 activation can take place. Erk1/2 might phosphorylate and activate IRF3 directly. Alternatively, Erk1/2 might activate IRF3 indirectly by phosphorylating TBK1, which has been recently identified as an IRF3 kinase[22,35,36]. Although the kinase IKKε also has the ability to phosphorylate IRF3, its expression is limited to the cells of lymphoid origin[22,35]. Or, finally, myxoma virus infection of nonpermissive pMEFs may specifically induce the expression of a previously unknown cellular Erk1/2 substrate that subsequently initiates IRF3 phosphorylation. These alternatives remain to be tested experimentally.

The critical function of IFN-STAT1 signaling identified as a cellular blockade to myxoma virus proliferation in this report raises an issue for future studies: why myxoma virus infection can elicit such a potent type I interferon response in nonpermissive pMEFs. In a set of preliminary experiments, we tested the induction of type I interferon in an array of various permissive transformed mouse cell lines. Myxoma virus was unable to induce type I interferon in all the permissive cells tested, whereas synthetic double-stranded RNA, poly(I:C), a widely used mimic for viral double-stranded RNA[18,39], was capable of eliciting a strong type I interferon response (data not shown). Thus, these results indicate that the yet-to-be-defined myxoma virus infection product that is distinct from double-stranded RNA is responsible for eliciting type I interferon induction and that only those cells that have the ability to recognize this new moiety as an initiator for the gene induction can mount a robust type I interferon response.

Erk1/2 is perhaps the most extensively described MAPK in mammalian cells. Increasing biological functions have been assigned to this ubiquitous signaling module[28,29,42,43]. In terms of viral infection, one fundamental issue is why myxoma virus–activated Erk1/2 participates in antiviral responses for the host, whereas Erk1/2 activated by other viruses such as influenza virus[10–12] is exploited for viral self-proliferation. Although there is no basis for direct comparison of the Erk1/2 signaling events in the myxoma virus–pMEF system with those in other viral systems, several key features documented for the Erk1/2 module are essential for understanding the functional importance of Erk1/2 signaling. It is now known that the outcome of a given Erk1/2 signaling cascade is both cell-type and stimulus specific[28,29,42,43]. For example, Erk1/2 signaling is often associated with cell differentiation. Phorbol 12-myristate 13-acetate elicits Erk1/2 activation in both U937 and UT16 cells, but phorbol 12-myristate 13-acetate–elicited Erk1/2 signaling induces differentiation only in U937 cells[8]. In another

example, both platelet-activating factor and tumor necrosis factor induce Erk1/2 activation in human airway smooth muscle cells, but only platelet-activating factor–induced Erk1/2 signaling is involved in RANTES expression[44]. Here, pMEFs were permissive for vaccinia virus replication, in contrast to the restrictive phenotype for myxoma virus. Vaccinia virus infection of pMEFs elicited robust Erk1/2 activation but with a distinctly different pattern, in that Elk1 became strongly phosphorylated (data not shown). Consequently, inactivation of vaccinia virus–induced Erk1/2 signaling with U0126 considerably inhibited vaccinia virus replication in pMEFs (data not shown). This result is consistent with a report that Erk1/2 activation is required for vaccinia virus infection in permissive transformed cells[13].

In conclusion, our observations here indicate an emerging theme that the signaling profile induced by an infecting virus is key in dictating the fate of virus-activated Erk1/2 signal flow and whether this pathway leads to type I interferon induction. Future characterization of which viral components determine the ultimate biological outcomes of an Erk1/2 signaling event should provide a new framework for investigating innate antiviral mechanisms in general.

METHODS

Mice, cell cultures, virus and reagents. Mice were housed and bred in a specific pathogen–free environment in the animal facility of the Washington University School of Medicine (St. Louis, Missouri). All animal experiments were reviewed and approved by the Washington University Animal Studies Committee and Institutional Biological & Chemical Safety Committee and were in compliance with federal, state and local laws and policies and with institutional guidelines. The pMEFs from *Ifnar1*$^{-/-}$, *Stat1*$^{-/-}$, *Prkr*$^{-/-}$ and *Stat1*$^{-/-}$*Prkr*$^{-/-}$ mice were on a 129Sv/Ev background[19,45,46], whereas *Prkr*$^{-/-}$*Rnasel*$^{-/-}$*Mx1*$^{-/-}$ pMEFs were on a C57BL/6 background[47]. Wild-type pMEFs of either genetic background were identical in terms of myxoma virus infectability. Myxoma virus (Lausanne strain) with or without a *lacZ* gene inserted at an innocuous intergenic site under the control of a late viral promoter has been described[30]. Myxoma virus was inactivated by ultraviolet irradiation with a Stratagene Stratalinker. All cell cultures were maintained in DMEM with 10% FBS. Cycloheximide, 5-bromo-4-chloro-3-indolyl-β-D-galactopyranoside (X-gal) and *o*-nitrophenyl-β-D-galactopyranoside were purchased from Sigma. Cytokines and immunodetection primary antibodies were from the following sources: mouse IFN-α, IFN-β, rabbit anti–mouse IFN-β and rat anti–mouse IFN-γ, Calbiochem; phospho-STAT1 (Y701), phospho-STAT1 (S727), phospho-Erk1/2 and Erk1/2, Upstate Biotechnology; phospho-PKR (T451), sheep anti–mouse IFN-α and IFN-β, Biosource International; phospho-Elk1, PKR and actin, Santa Cruz Biotechnology; phospho-eIF2α (S51), p38 and Jnk, Cell Signaling Technology; and IRF3, Zymed. Rabbit antibody to myxoma virus antigen M-T7 has been described[30].

Virus infection, inhibitor and neutralization experiments, antisense 'knockdown', and enzyme-linked immunosorbent assay (ELISA). Myxoma virus was used at a MOI of 0.01 for plaque assays by X-gal staining at 48 h after infection and a MOI of 1.0 for RT-PCR, immunoblot, immunofluoresence and ELISA for various times as indicated in **Figures 1,3–7**. Myxoma virus replication–mediated β-gal assays used *o*-nitrophenyl-β-D-galactopyranoside as described[48] and the 'fold increase' of the β-gal activity in various myxoma virus infection conditions is expressed relative to that of myxoma virus infection alone. The MEK inhibitor U0126 (Promega) was included at a concentration of 30 μM in the culture medium 30 min before the infection was initiated and the concentration was maintained throughout the whole infection period. The same treatment procedure was used for cycloheximide (50 μg/ml) where indicated in **Figure 1d**. For neutralization experiments, anti–IFN-α and IFN-β or anti–IFN-γ was added to the medium 2 h before the viral challenge and each was maintained throughout the infection at a dose of 1,000 neutralization units/ml. For experiments with exogenous mouse IFN-α and IFN-β, the cytokines were added at a concentration of 50 units/ml to the medium when myxoma virus infection was started. For the Erk1/2 antisense 'knockdown'

experiment, the 17-residue phosphorothioate oligodeoxynucleotide directed against the consensus sequence of both the Erk1 and Erk2 isoforms and its corresponding scrambled control oligodeoxynucleotide were obtained from Calbiochem. Intracellular delivery of the oligodeoxynucleotides at various concentrations was accomplished according to the product specifications. At 60 h after the delivery, oligodeoxynucleotide-treated pMEFs were used to verify Erk1/2 protein expression by immunoblot or to define myxoma virus infectivity by plaque assay with X-gal staining. All X-gal microscopic images were obtained at a magnification of ×50 with a Zeiss Axioskop microscope. For the *in vivo* experiments, age- and sex-matched mice were infected intracranially with various myxoma virus doses (**Fig. 8**) at 8–12 weeks of age and were monitored for survival for 21 d after infection. The intracranial infection procedure has been described[49].

For quantification of IFN-β produced after myxoma virus infection of pMEFs with or without U0126 pretreatment, supernatants were collected 24 h after infection and were assessed by standard sandwich ELISA as described[50]. For demonstration of the antiviral activity of type I interferon in the pMEFs used here, the cells were pretreated with increasing concentrations of the cytokine for 24 h as indicated in **Figure 2e** and then were exposed to vesicular stomatitis virus. The cytopathic assays were done as described by measurement of uptake of the vital dye crystal violet at 540 nm (ref. 46).

RT-PCR. Monolayers of pMEFs grown in 25-cm² flasks were infected with myxoma virus. At various times after infection (**Figs. 3b,c** and **5c,d**), the cells were lysed and total RNA was isolated with a RNeasy kit (Qiagen). Reverse transcription was done with Superscript reverse transcriptase (Gibco BRL). The primer sequences for mouse IFN-β, universal IFN-α (consensus sequence annealing with all known subtypes of IFN-α), delayed IFN-α (sequence annealing only with non-IFN-α4 subtypes of IFN-α), IRF3, IRF7 and glyceraldehyde phosphodehydrogenase as well as the RT-PCR conditions have been described[38].

Immunofluorescence microscopy. For immunofluorescence experiments, pMEFs were grown on coverslips. After infection with myxoma virus for 12 h, the infected cells were fixed in cold methanol for 5 min, washed in PBS and blocked in 2% BSA. For double staining of phospho-Erk1/2 and M-T7, mouse monoclonal antibody to phospho-Erk1/2 and rabbit polyclonal antibody to M-T7 were applied at 25 °C for 1 h followed by a 50-minute secondary detection with Texas Red–conjugated goat anti-mouse IgG and fluorescein isothiocyanate–conjugated goat anti-rabbit IgG, respectively. For single staining of M-T7 or IRF3, myxoma virus–infected pMEFs were incubated for 1 h with corresponding primary antibodies and were visualized either with fluorescein isothiocyanate–conjugated goat anti-rabbit IgG or with Texas Red–conjugated goat anti-rabbit IgG as indicated in **Figures 1e**, **3d** and **5b**. All secondary antibody conjugates were from Jackson ImmunoResearch Laboratories. Fluorescence images were obtained with a Leica DMIRE2 microscope.

Immunoblots. The pMEFs were grown in 25-cm² flasks and were infected with myxoma virus for various times as indicated in **Figures 1d**, **4a–c**, **5a**, **6a,d,f** and **7c**. At each specified time after infection, whole-cell extracts were prepared with radioimmunoprecipitation assay lysis buffer supplemented with protease and phosphatase inhibitors from the complete protease inhibitor 'cocktail' tablet (Roche Diagnostics) and phosphatase inhibitor 'cocktail' I and II (Sigma) according to the manufacturers' specification. Total cellular proteins were resolved by 7.5–12% SDS-PAGE and were transferred to Hybond-C nitrocellulose (Amersham Pharmacia Biotech). Immunoblots were done with the respective primary antibodies, and bands were visualized with secondary horseradish peroxidase–conjugated antibodies and the ECL system (NEN Life Science Products).

COMPETING INTERESTS STATEMENT
The authors declare that they have no competing financial interests.

1. Esposito, J.J. & Fenner, F. in *Fields Virology* 4th edn. (eds. Knipe, D.M. & Howley, P.M.) 2885–2921 (Lippincott Williams & Wilkins, Philadelphia, 2001).
2. Fenner, F. & Ratcliffe, F.N. *Myxomatosis* (Cambridge University Press, Cambridge, UK, 1965).
3. Kerr, P. & McFadden, G. Immune responses to myxoma virus. *Viral Immunol.* **15**, 229–246 (2002).
4. Moss, B. in *Fields Virology* 4th edn. (eds. Knipe, D.M. & Howley, P.M.) 2849–2883 (Lippincott Williams & Wilkins, Philadelphia, 2001).
5. Lalani, A.S. *et al.* Use of chemokine receptors by poxviruses. *Science* **286**, 1968–1971 (1999).
6. Johnston, J.B. *et al.* Role of the serine-threonine kinase PAK-1 in myxoma virus replication. *J. Virol.* **77**, 5877–5888 (2003).
7. Condit, R.C. in *Fields Virology* 4th edn. (eds. Knipe, D.M. & Howley, P.M.) 19–51 (Lippincott Williams & Wilkins, Philadelphia, 2001).
8. Rao, K.M.K. MAP kinase activation in macrophages. *J. Leukoc. Biol.* **69**, 3–10 (2001).
9. Greber, U.F. Signaling in viral entry. *Cell. Mol. Life Sci.* **59**, 608–626 (2002).
10. Planz, O., Pleschka, S. & Ludwig, S. MEK-specific inhibitor U0126 blocks spread of Borna disease virus in cultured cells. *J. Virol.* **75**, 4871–4877 (2001).
11. Pleschka, S. *et al.* Influenza virus propogation is impaired by inhibition of the Raf/MEK/ERK signalling cascade. *Nat. Cell Biol.* **3**, 301–305 (2001).
12. Luo, H. *et al.* Coxsackievirus B3 replication is reduced by inhibition of the extracellular signal-regulated kinase (ERK) signaling pathway. *J. Virol.* **76**, 3365–3373 (2002).
13. Andrade, A.A. *et al.* The vaccinia virus-stimulated mitogen-activated protein kinase (MAPK) pathway is required for virus multiplication. *Biochem. J.* **381**, 437–446 (2004).
14. Booth, J.L., Coggeshall, K.M., Gordon, B.E. & Metcalf, J.P. Adenovirus type 7 induces interleukin-8 in a lung slice model and requires activation of Erk. *J. Virol.* **78**, 4156–4164 (2004).
15. Mainiero, F. *et al.* Integrin-mediated Ras-extracellular regulated kinase (ERK) signaling regulates interferon γ production in human natural killer cells. *J. Exp. Med.* **188**, 1267–1275 (1998).
16. Egerton, M., Fitzpatrick, D.R. & Kelso, A. Activation of the extracellular signal-regulated kinase pathway is differentially required for TCR-stimulated production of six cytokines in primary T lymphocytes. *Int. Immunol.* **10**, 223–229 (1998).
17. Popik, W., Hesselgesser, J.E. & Pitha, P.M. Binding of human immunodeficiency virus type 1 to CD4 and CXCR4 receptors differentially regulates expression of inflammatory genes and activates the MEK/ERK signaling pathway. *J. Virol.* **72**, 6406–6413 (1998).
18. Samuel, C.E. Antiviral actions of interferons. *Clin. Microbiol. Rev.* **14**, 778–809 (2001).
19. Müller, U. *et al.* Functional role of type I and type II interferons in antiviral defense. *Science* **264**, 1918–1921 (1994).
20. Levy, D.E. & Darnell Jr., J.E. STATS: Transcriptional control and biological impact. *Nat. Rev. Mol. Cell Biol.* **3**, 651–662 (2002).
21. Levy, D.E., Marié, I., Smith, E. & Prakash, A. Enhancement and diversification of IFN induction by IRF-7-mediated positive feedback. *J. Interferon Cytokine Res.* **22**, 87–93 (2002).
22. Sharma, S. *et al.* Triggering the interferon antiviral response through an IKK-related pathway. *Science* **300**, 1148–1151 (2003).
23. Katze, M.G., He, Y. & Gale Jr., M. Viruses and interferon: a fight for supremacy. *Nat. Rev. Immunol.* **2**, 675–687 (2002).
24. Taniguchi, T., Ogasawara, K., Takaoka, A. & Tanaka, N. IRF family of transcription factors as regulators of host defense. *Annu. Rev. Immunol.* **19**, 623–655 (2001).
25. Peters, K.L., Smith, H.L., Stark, G.R. & Sen, G.C. IRF-3-dependent, NFκB- and JNK-independent activation of the 561 and IFN-β genes in response to double-stranded RNA. *Proc. Natl. Acad. Sci. USA* **99**, 6322–6327 (2002).
26. Favata, M.F. *et al.* Identification of a novel inhibitor of mitogen-activated protein kinase kinase. *J. Biol. Chem.* **273**, 18623–18632 (1998).
27. Brunet, A. *et al.* Nuclear translocation of p42/p44 mitogen-activated protein kinase is required for growth factor-induced gene expression and cell cycle entry. *EMBO J.* **18**, 664–674 (1999).
28. Widmann, C., Gibson, S., Jarpe, M.B. & Johnson, G.L. Mitogen-activated protein kinase: conservation of a three-kinase module from yeast to human. *Physiol. Rev.* **79**, 143–180 (1999).
29. Pouysségur, J., Volmat, V. & Lenormand, P. Fidelity and spatio-temporal control in MAP kinase (ERKs) signalling. *Biochem. Pharmacol.* **64**, 755–763 (2002).
30. Mossman, K. *et al.* Myxoma virus M-T7, a secreted homolog of the interferon-γ receptor, is a critical virulence factor for the development of myxomatosis in European rabbits. *Virology* **215**, 17–30 (1996).
31. Sale, E.M., Atkinson, P.G.P. & Sale, G.J. Requirement of MAP kinase for differentiation of fibroblasts to adipocytes, for insulin activation of p90 S6 kinase and for insulin or serum stimulation of DNA synthesis. *EMBO J.* **14**, 674–684 (1995).
32. Robinson, C.J.M. *et al.* Treatment of vascular smooth muscle cells with antisense phosphorothioate oligodeoxynucleotides directed against p42 and p44 mitogen-activated protein kinases abolishes DNA synthesis in response to platelet-derived growth factor. *Biochem. J.* **320**, 123–127 (1996).
33. Stark, G.R., Kerr, I.M., Williams, B.R.G., Silverman, R.H. & Schreiber, R.D. How cells respond to interferons. *Annu. Rev. Biochem.* **67**, 227–264 (1998).

34. David, M. *et al.* Requirement for MAP kinase (ERK2) activity in interferon α- and interferon β-stimulated gene expression through STAT proteins. *Science* **269**, 1721–1723 (1995).

35. McWhirter, S.M., Fitzgerald, K.A., Rosains, J., Rowe, D.C. & Golenbock, D.T. IFN-regulatory factor 3-dependent gene expression is defective in *Tbk1*-deficient mouse embryonic fibroblasts. *Proc. Natl. Acad. Sci. USA* **101**, 233–238 (2004).

36. Fitzgerald, K.A. *et al.* IKKε and TBK1 are essential components of the IRF3 signaling pathway. *Nat. Immunol.* **4**, 491–496 (2003).

37. Smith, E.J., Marié, I., Prakash, A., García-Sastre, A. & Levy, D.E. IRF3 and IRF7 phosphorylation in virus-infected cells does not require double-stranded RNA-dependent protein kinase R or IκB kinase but is blocked by vaccinia virus E3L protein. *J. Biol. Chem.* **276**, 8951–8957 (2001).

38. Marié, I., Durbin, J.E. & Levy, D.E. Differential viral induction of distinct interferon-α genes by positive feedback through interferon regulatory factor-7. *EMBO J.* **17**, 6660–6669 (1998).

39. Jacobs, B.L. & Langland, J.O. When two strands are better than one: the mediators and modulators of the cellular responses to double-stranded RNA. *Virology* **219**, 339–349 (1996).

40. Williams, B.R.G. PKR; a sentinel kinase for cellular stress. *Oncogene* **18**, 6112–6120 (1999).

41. Schneider-Schaulies, J. Cellular receptors for viruses: links to tropism and pathogenesis. *J. Gen. Virol.* **81**, 1413–1429 (2000).

42. Pearson, G. *et al.* Mitogen-activated protein (MAP) kinase pathways: regulation and physiological functions. *Endocr. Rev.* **22**, 153–183 (2001).

43. Schaeffer, H.J. & Weber, M.J. Mitogen-activated protein kinases: specific messages from ubiquitous messengers. *Mol. Cell. Biol.* **19**, 2435–2444 (1999).

44. Maruoka, S., Hashimoto, S., Gon, Y., Takeshita, I. & Horie, T. PAF-induced RANTES production by human airway smooth muscle cells requires both p38 MAP kinase and Erk. *Am. J. Respir. Crit. Care Med.* **161**, 922–929 (2000).

45. Yang, Y.L. *et al.* Deficient signaling in mice devoid of double-stranded RNA-dependent protein kinase. *EMBO J.* **14**, 6095–6106 (1995).

46. Meraz, M.A. *et al.* Targeted disruption of the *Stat1* gene in mice reveals unexpected physiologic specificity in the JAK-STAT signaling pathway. *Cell* **84**, 431–442 (1996).

47. Zhou, A., Paranjape, J.M., Der, S.D., Williams, B.R.G. & Silverman, R.H. Interferon action in triply deficient mice reveals the existence of alternative antiviral pathways. *Virology* **258**, 435–440 (1999).

48. Li, Y., Hall, R.L. & Moyer, R.W. Transient, nonlethal expression of genes in vertebrate cells by recombinant entomopoxviruses. *J. Virol.* **71**, 9557–9562 (1997).

49. van Berkel, V. *et al.* Critical role for a high-affinity chemokine-binding protein in γ-herpesvirus-induced lethal meningitis. *J. Clin. Invest.* **109**, 905–914 (2002).

50. Asselin-Paturel, C. *et al.* Mouse type I IFN-producing cells are immature APCs with plasmacytoid morphology. *Nat. Immunol.* **2**, 1144–1150 (2001).